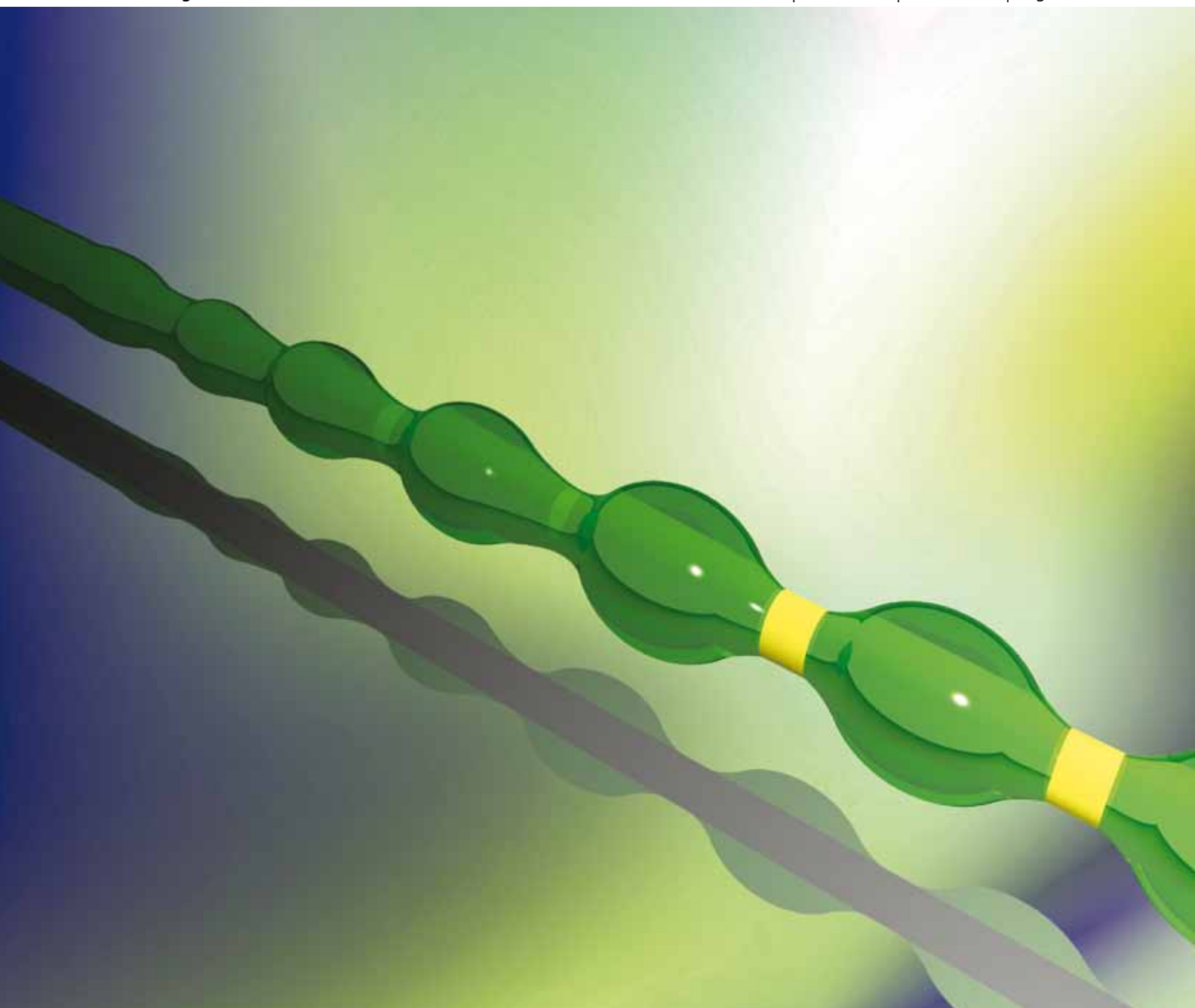


Soft Matter

www.softmatter.org

Volume 5 | Number 11 | 7 June 2009 | Pages 2145–2324



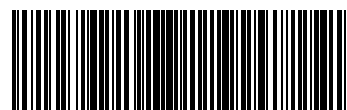
ISSN 1744-683X

PAPER

Mohan Srinivasarao *et al.*
Non-classical scaling for forced
wetting of a nematic fluid on a
polymeric fiber

REVIEW

Josef A. Käs *et al.*
Passive and active single-cell
biomechanics: a new perspective in
cancer diagnosis



1744-683X(2009)5:11;1-5

RSC Publishing

Non-classical scaling for forced wetting of a nematic fluid on a polymeric fiber

Jung Ok Park,^{ab} Alejandro D. Rey^c and Mohan Srinivasarao^{*abd}

Received 17th June 2008, Accepted 24th December 2008

First published as an Advance Article on the web 10th February 2009

DOI: 10.1039/b808411d

We report on the forced wetting of a liquid crystal on a polymer fiber in the nematic and isotropic phase under partial wetting conditions. As the cylindrical fiber exits from the fluid reservoir, the fluid forced-coated on the fiber is immediately broken into droplets due to capillary-driven instability, even in the wetting conditions. For the nematic fluid, the initial film thickness, h , before breakup, scales almost linearly with the capillary number, Ca , as $h \sim Ca^{0.94}$, while $h \sim Ca^{2/3}$ for the isotropic fluid, as predicted for a Newtonian fluid. The amount of the fluid coated on a fiber is larger in the nematic phase than in the isotropic phase at a given velocity within the velocity range studied. Analysis using Ericksen-Leslie equations shows that Frank elasticity plays no role in increasing the coating thickness for the nematic fluid, while viscous anisotropy is the source of observed rescaling, $h \sim Ca$. This non-classical scaling is attributed to the deformation-stress cross-coupling and the existence of extensional kinematics in the meniscus formation region.

Introduction

In many industrial applications it is necessary to coat a solid substrate with a fluid for a variety of reasons.^{1–6} This is usually accomplished by dragging the solid object through the fluid of interest. Here we refer to such processes as forced wetting of the solid substrate, irrespective of whether the fluid is a wetting or a nonwetting fluid for the substrate. In such a process, it is obvious that the thickness of the fluid coating will depend on the velocity at which the solid substrate is withdrawn. At zero velocity the film thickness is zero (where we ignore the possibility of a thin wetting film), and at infinite velocity it will be zero as well since the fluid does not have enough time to form a coating and/or the air is entrapped in the interface. Thus a maximum wetting speed naturally enters the problem of forced wetting.^{7–12}

We are interested in gaining an understanding of how the fluid film thickness varies with an increase in velocity. In particular, we confine our attention to the special case of the solid substrate having a cylindrical geometry and where the fluid is an anisotropic fluid with long range orientational order. The wetting and spreading characteristics of nematic fluids on planar substrates have been extensively studied,^{13–19} while the behavior on cylindrical objects has hardly been studied. In this letter, we report on the forced spreading of a nematic fluid on a polypropylene fiber, both in its ordered and disordered phase.

The wettability of a dry ideal solid by a liquid is determined by the spreading coefficient, S , which is defined as $S = \gamma_s - \gamma_{sl} - \gamma$,

where γ_s , γ_{sl} , and γ are surface energy of the substrate, substrate–liquid interfacial tension, and surface tension of the liquid, respectively.^{11,20} The spreading coefficient is the difference between the surface energy of the dry solid surface, γ_s , and the interfacial energy of a wetted surface, $\gamma_{sl} + \gamma$. When $S > 0$, a fluid drop will spontaneously spread on a planar surface because the wetted surface has a lower free energy than the dry surface, and this is referred to as total wetting or spontaneous wetting. When $S < 0$, the fluid partially wets the surface such that there is a finite contact angle, θ , with $S = \gamma(-1 + \cos \theta)$.

Wetting of cylindrical substrates, or fibers, by viscous fluids differs from that of planar substrates of the same material. This is due to the fact that the curvature of the fiber causes capillary pressure imbalance at two interfaces of the annular fluid film, namely the substrate–fluid and the air–fluid interfaces. An important consequence is that fiber wetting occurs only when the spreading parameter S is greater than a critical *positive* value, S_c ,^{21–27} while wetting on planar substrates occurs when $S > 0$. In many cases, this annular film is quickly broken into droplets^{21–23,26,28} due to Rayleigh instability.²⁹ Under the same conditions, the film thickness before breakup is greater for fibers than for planar substrates.³⁰

Nonslip boundary conditions coupled with the finite viscosity of the fluid lead to the result that the fluid elements near the solid must move at the same velocity as that of the solid, forming a thin coating on the fiber. However, this motion results in a deformation of the fluid–air interface, which is opposed by surface tension forces. Hence, viscous and capillary forces oppose each other, thereby naturally introducing a force balance defined by the ratio between the two, the so-called capillary number, Ca ($Ca = \eta V/\gamma$), where η is the fluid viscosity. It is expected that the initial film thickness, h , can be expressed as $h \sim l f(Ca)$, where l is some static length which will depend on the geometry of the solid. Landau, Levich and Derjaguin were the first to correctly predict that the film thickness at low withdrawal velocity will scale as $h \sim Ca^{2/3}$ for Newtonian

^aSchool of Polymer Textile and Fiber Engineering, Georgia Institute of Technology, Atlanta, GA, 30332-0295, USA. E-mail: jung.park@ptfe.gatech.edu

^bCenter for Advanced Research on Optical Microscopy, Georgia Institute of Technology, Atlanta, GA, 30332-0295, USA

^cDepartment of Chemical Engineering, McGill University, Montreal/Quebec, H3A 2B2, Canada. E-mail: alejandro.rey@mcgill.ca

^dSchool of Chemistry and Biochemistry, Georgia Institute of Technology, Atlanta, GA, 30332-0400, USA. E-mail: mohan@ptfe.gatech.edu

fluids.^{31,32} This is the well-known LLD law for free meniscus coating.

Nematic liquid crystals have long-range orientational order without positional order, and the average molecular orientation is given by a unit vector, the director \mathbf{n} . The fiber wetting by nematics involves the determination of director orientation in annular spaces.^{33,34} For nematic liquid crystals, the Frank elasticity due to orientation gradients may have to be taken into account, depending on their significance in comparison to the viscous stress.

Experimental section

We have used a eutectic liquid crystal mixture, E7, in the nematic phase (at room temperature) and in the isotropic phase (at 100 °C). E7 is composed of K15 (4-pentyl-4'-cyanobiphenyl), K21 (4-heptyl-4'-cyanobiphenyl), M24 (4-octyloxy-4'-cyanobiphenyl), and T15 (4-pentyl-4'-cyanoterphenyl), and is a homogenous mixture (single thermodynamic phase) with a single nematic–isotropic transition temperature of 60–61 °C.^{35,36} A polypropylene fiber of diameter 200 μm is dragged through a Teflon tube reservoir (inner radius = 0.24 cm, length = 1.5 cm) containing E7. The fiber passes through the tube in the horizontal direction at a constant velocity, V , and the mass of this fluid reservoir is continuously recorded as a function of time, t . As the fiber moves through the reservoir, the mass of the fluid uptake by the fiber, ΔW , increases linearly with time. As mentioned above, the annular liquid film forced-wet breaks up, but the initial film thickness, h , can be easily computed using the mass balance equation:

$$h = -r + \left(r^2 + \frac{\Delta W / \Delta t}{\pi \rho V} \right)^{1/2},$$

where r and ρ are the fiber radius and fluid density.

Results and discussion

The forced wetting of E7 nematic liquid crystal on PP fiber quickly reaches the steady state and the weight pickup is linear in time, as shown in Fig. 1 for several withdrawal velocities. We

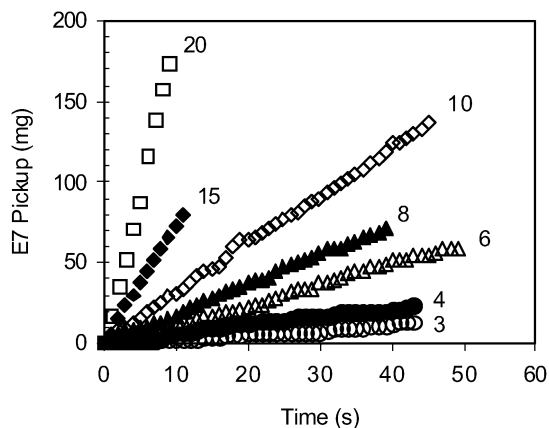


Fig. 1 The amount of the nematic E7 liquid crystal picked up by a polypropylene fiber at various velocities (as indicated in the graph in cm s⁻¹) at room temperature.

stress here that the thickness, calculated using aforementioned mass balance, is just the initial thickness, largely because the annular fluid is unstable and breaks up by the surface-tension-driven “Rayleigh Instability”. We do not report the dynamics of this instability in this paper; this will be discussed elsewhere.

Fig. 2 is a bilogarithmic plot of the reduced thickness, h/r , of the nematic E7 fluid as a function of capillary number, corresponding to velocities of the fiber ranging from 2 to 25 cm s⁻¹. The fluid film thickness is seen to be much larger and to scale with a higher exponent ($h/r \sim Ca^{0.94}$) than predicted by the LLD law of $h/r \sim Ca^{2/3}$. It must be emphasized that the viscosity of the nematic fluid is expected to be independent of the shear rate (2560–3180 s⁻¹) in the range of fiber withdrawal velocities studied.

On the other hand, when the fluid is heated to 100 °C by an infrared heater to induce phase transition of E7 from nematic to isotropic state, the dependence of the thickness on the velocity exactly follows the LLD prediction, as shown in Fig. 3.

To determine the driving force behind the new scaling law in nematic phase, the anisotropic viscoelastic nature of nematic liquid crystals must be taken into account. *Anisotropic elasticity*, generally known as Frank elasticity, is due to three modes of

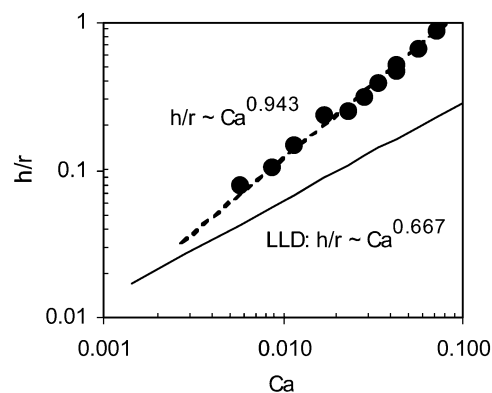


Fig. 2 The reduced thickness, h/r , of the nematic E7 on polypropylene fiber at room temperature as a function of the capillary number. The thickness increases much faster than the LLD law predicts.

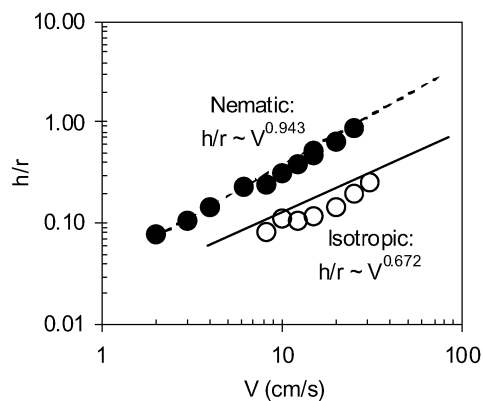


Fig. 3 The reduced thickness, h/r , of the E7 fluid on polypropylene fiber, both in nematic phase (at 25 °C) and isotropic phase (at 100 °C) as a function of velocity. The E7 at isotropic phase follows the prediction by LLD.

orientation gradient, namely splay, bend, and twist. Anisotropic viscosity implies that the viscosity is an orientation-dependent fourth-order tensor, and even a simple shear flow can generate different dissipation according to the nematic orientation. Determining the nature of driving force behind the new scaling law requires first assessing the relative importance of elasticity and viscosity, and then analyzing the specific nature of the anisotropy. The relative strength of viscous to elastic stresses is given by the Ericksen number,^{37–39} Er , as $Er = \eta Vh/K$,⁴⁰ where K is a characteristic Frank elastic constant. Using characteristic value of $K \sim 10^{-7}$ dyne,⁴¹ $Er = 10^3$ – 10^5 for the experimental velocity and film thickness range. Since the Ericksen number is greater than 1, *orientation-dependent elasticity is not the source of the new scaling*. However, we need to take orientation-dependent viscosity into consideration, as discussed below.

The non-viscometric kinematics of forced wetting, as shown in Fig. 4, consists of a non-homogeneous mixture of shear and extensional deformations. For simplicity we analyze the problem in rectangular coordinates. Assume that a fiber of radius r moves in the x direction with velocity V , and that h is the film thickness in the y direction that forms in a length given by λ . The characteristic velocity in the y direction is U . Assuming incompressibility, it follows that $V/\lambda \sim U/h$ and hence $U \sim Vh/\lambda$. Describing forced wetting with a two dimensional shear-extensional flow, the symmetric traceless rate of deformation tensor \mathbf{A} may be expressed in the extensional deformation term, A_{xx} , and the shear deformation term, A_{xy} . From the geometry of forced wetting, the deformations scale as: $A_{xx} \sim V/\lambda$, $A_{yx} = A_{xy} \sim V/h + U/\lambda \sim V/h + Vh/\lambda^2$, $A_{yy} \sim U/h \sim V/\lambda$.

Given the scales of the kinematics, the nature of generated viscous stresses is determined by the structure of the fluid. Newtonian fluids generate shear stresses with shear deformations and normal stresses with extensional deformations, and therefore exhibit no cross-coupling between the type of deformation and the type of stress.

On the other hand, the anisotropic viscous nature of nematic liquid crystals allows for cross-couplings between stress and deformation, such that shear may generate shear and normal stresses, while extensional flow generates shear and normal stresses. The simplest theory that captures anisotropic viscous behavior is the following transversely isotropic fluid (TIF) Ericksen model:^{37–39,42,43}

$$\mathbf{t} = \eta_1 \mathbf{A} : \mathbf{n} \mathbf{n} \mathbf{n} \mathbf{n} + 2\eta_2 \mathbf{A} + \eta_3 (\mathbf{A} \cdot \mathbf{n} \mathbf{n} + \mathbf{n} \mathbf{n} \cdot \mathbf{A}) \quad (1)$$

where \mathbf{t} is the symmetric stress tensor, and the η_1 , η_2 , and η_3 are orientation-dependent viscosities. Note that for a Newtonian

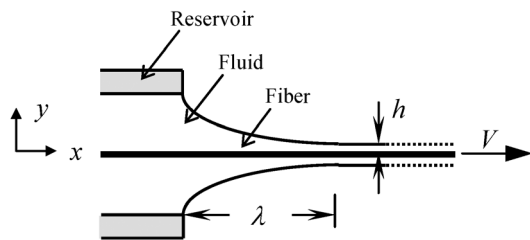


Fig. 4 A sketch of the dynamic meniscus, where h is the thickness of the liquid layer and λ is the length over which the film is formed at a given velocity.

fluid $\eta_1 = \eta_3 = 0$. The relevant stress tensor components are the shear stress $t_{yx} = t_{xy}$, and the normal stresses t_{xx} and t_{yy} . For the TIF fluid, these are given by

$$t_{xy} = t_{yx} = [\eta_1(n_x^2 - n_y^2)n_x n_y]A_{xx} + [2\eta_1 n_x^2 n_y^2 + 2\eta_2 + \eta_3]A_{xy} \quad (2a)$$

$$t_{xx} = [\eta_1(n_x^2 - n_y^2)n_x^2 + 2\eta_2 + 2\eta_3 n_x^2]A_{xx} + [2\eta_1 n_x^3 n_y + 2\eta_3 n_x n_y]A_{xy} \quad (2b)$$

$$t_{yy} = [\eta_1(n_x^2 - n_y^2)n_y^2 - 2\eta_2 - 2\eta_3 n_y^2]A_{xx} + [2\eta_1 n_x n_y^3 + 2\eta_3 n_x n_y]A_{xy} \quad (2c)$$

where we have used $A_{xx} = -A_{yy}$ and $A_{xy} = A_{yx}$. The above equations show that, for this complex fluid, shear deformation contributes to shear and normal stresses and extensional deformation also contributes to shear and normal stresses, clearly identifying the stress-deformation coupling.

Integrating the linear momentum balance in the y direction gives:

$$(t_{yy} - p) - (t_{yy} - p)|_h - \int_y^h t_{xy,x} dy = 0 \quad (3)$$

Since, at $y = h$, the normal stress t_{yy} is balanced by the Laplace pressure, $(t_{yy} - p)|_h = \gamma(d^2h/dx^2)$, the pressure and its axial gradient are:

$$-p_x = t_{yy,x} + \gamma h_{xx} + \int_y^h t_{xy,x} dy \quad (4)$$

Replacing the pressure gradient into the x -component of the linear momentum balance equation gives:

$$-\gamma \frac{\partial^3 h}{\partial x^3} = \frac{\partial t_{yx}}{\partial y} + \frac{\partial N_1}{\partial x} + \frac{\partial}{\partial x} \int_y^h t_{xy} dy \quad (5)$$

where $N_1 (= t_{xx} - t_{yy})$ is the first normal stress difference. Capillary forces are balanced by shear and normal stresses. The normal stress forces arise through axial gradients while shear stress forces through transverse and axial gradients.

The characteristic values of these stresses are obtained by using V as the velocity scale, h as the length scale in the thickness (y) direction, λ as the length scale in the flow (x) direction, and the continuity equation ($U \sim Vh/\lambda$):

$$t_{xy} = \alpha_1^*(V/\lambda) + \alpha_2^*(V/h) + \alpha_3^*(Vh/\lambda^2) \quad (6)$$

$$N_1 = \alpha_4^*(V/\lambda) + \alpha_5^*(V/h) + \alpha_6^*(Vh/\lambda^2) \quad (7)$$

where the coefficients $\{\alpha_i^*; i = 1-6\}$ are the characteristic viscosity functions of the bare viscosities $\{\eta_1, \eta_2, \eta_3\}$. The cross-couplings are introduced by α_1^* , α_5^* , α_6^* , and from equations (2) it is seen that they do not vanish unless the unlikely conditions $n_x = 0$ or $n_y = 0$ hold everywhere. For Newtonian fluids, the cross-couplings are always zero. The characteristic values of the force balance equation in the flow direction are:

$$\gamma h/\lambda^3 = \alpha_2^*(V/h^2) + \alpha_{145}^*(V/\lambda h) + \alpha_{23}^*(V/\lambda^2) + \alpha_{16}^*(Vh/\lambda^3) + \alpha_3^*(Vh^2/\lambda^4) \quad (8)$$

where $\alpha_{145}^* = \alpha_1^* + \alpha_4^* + \alpha_5^*$ and $\alpha_{23}^* = \alpha_2^* + \alpha_3^*$, and $\alpha_{16}^* = \alpha_1^* + \alpha_6^*$. The film development length λ is found from the

balance between the two curvature-induced capillary pressures, $[\gamma/(r+h)] - (\gamma h/\lambda^2) = 0$, and yields $\lambda = [h(r+h)]^{1/2}$. More general models may also take into account the effect of normal stress on λ , but for the present case we use the simplest possible model. Introducing the capillary number and the expression for λ in equation (8), we find for $h/r \ll 1$:

$$Ca = (h/r)^{3/2}[\alpha_{145}^*(h/r)^{1/2} + \alpha_{23}^*(h/r) + \alpha_2^* + \alpha_{16}^*(h/r)^{3/2} + \alpha_3^*(h/r)^2]^{-1} \quad (9)$$

A number of observations follow from equation (9). First, for low-molar mass Newtonian fluids, the equation (9) goes back to the LLD law, because stress-deformation cross-couplings do not exist ($\alpha_1^* = \alpha_5^* = \alpha_6^* = 0$), and because normal stresses from extensional deformations are negligible ($\alpha_4^* = 0$). Second, for nematic liquid crystals, the corresponding coefficients are not zero since cross-couplings and normal stresses also contribute, and hence the LLD law is not obeyed. Third, the viscosity functions α_{145}^* , α_{23}^* , and α_{16}^* do not affect the power law scaling.

Rearranging equation (9) gives equation (10), where the coating thickness scales linearly with the capillary number.

$$Ca = (h/r)^{3/2}[\alpha_{145}^*(h/r)^{1/2}]^{-1}[1 + \dots]^{-1} = \alpha_{145}^* h/r + \dots \quad (10)$$

Thus, the Ericksen model is consistent with the observed scaling. The power law scaling arises from the stress-deformation laws for nematic liquid crystals, which introduce *cross-couplings and normal stresses not observed in Newtonian materials*.

Conclusions

Forced wetting experiments have been carried out and measurements of coating thickness of a typical nematic liquid crystal on a polymeric fiber show that the classical LLD scaling of the coating thickness with the capillary number does not hold for anisotropic fluid. The measured dependence for E7 is $h/r \sim Ca^{0.94}$ in the nematic phase, while it is $h/r \sim Ca^{2/3}$ in the isotropic state as predicted by LLD. Analysis of the experiment using classical liquid crystal physics shows that orientation elasticity plays no role in the exponent's rescaling. Viscous anisotropy in nematic liquid crystals is shown to be the source of rescaling, $h/r \sim Ca$, through the presence of deformation-stress cross-coupling and through the existence of extensional kinematics in the meniscus formation region.

Acknowledgements

Srinivasarao acknowledges the support from NSF (DMR-637233 and DMR-706235). Rey acknowledges support from the ACS-Petroleum Research Fund.

References

- 1 K. J. Ruschak, *Annual Review of Fluid Mechanics*, 1985, **17**, 65–89.
- 2 G. F. Teletzke, H. T. Davis and L. E. Scriven, *Revue de Physique Appliquee*, 1988, **23**, 989–1007.

- 3 *Coatings Technology Handbook*, ed. D. Satas, Marcel Dekker, New York, 2000, p. 679.
- 4 *Coatings technology Handbook*, ed. A. A. Tracton, Marcel Dekker, New York, 2005, p. 679.
- 5 *Coatings of Polymers and Plastics*, ed. R. A. Ryntz and P. V. Yaneff, Marcel Dekker, New York, 2003, p. 121.
- 6 *Plastics Finishing and Decoration*, ed. D. Satas, Van Nostrand Reinhold, New York, 1986, p. 113.
- 7 D. Quere, *Annual Review of Fluid Mechanics*, 1999, **31**, 347–384.
- 8 T. D. Blake and K. J. Ruschak, *Nature*, 1979, **282**, 489–491.
- 9 T. D. Blake, R. A. Dobson and K. J. Ruschak, *Journal of Colloid and Interface Science*, 2004, **279**, 198–205.
- 10 B. S. Kennedy and R. Burley, *Journal of Colloid and Interface Science*, 1977, **62**, 48–62.
- 11 P. G. de Gennes, *Reviews of Modern Physics*, 1985, **57**, 827–863.
- 12 M. N. Esmail and M. T. Ghannam, *Canadian Journal of Chemical Engineering*, 1990, **68**, 197–203.
- 13 B. Jerome and M. Boix, *Physical Review A*, 1992, **45**, 5746–5759.
- 14 B. Jerome and M. Boix, *Europhysics Letters*, 1992, **17**, 169–174.
- 15 M. M. T. Dagama, *Molecular Physics*, 1984, **52**, 611–630.
- 16 L. M. Blinov and V. G. Chirinov, Springer-Verlag, New York, 1994, pp. 97–131.
- 17 B. Jerome and P. Pieranski, *Liquid Crystals*, 1989, **5**, 683–691.
- 18 B. Jerome and P. Pieranski, *Journal de Physique*, 1988, **49**, 1601–1613.
- 19 A. A. Sonin, *The Surface Physics of Liquid Crystals*, Gordon and Breach Publishers, Amsterdam, 1995, pp. 59–70.
- 20 A. W. Adamson and A. P. Gast, *Physical Chemistry of Surfaces*, John Wiley and Sons, New York, 1997, p. 465.
- 21 F. Brochard-Wyart, J. M. Dimeglio and D. Quere, *Journal de Physique*, 1990, **51**, 293–306.
- 22 F. Brochard-Wyart and J. M. Dimeglio, *Annali Di Chimica*, 1987, **77**, 275–283.
- 23 F. Brochard-Wyart, *Comptes Rendus de l'Academie des Sciences, Serie II*, 1986, **303**, 1077–1080.
- 24 F. Brochard, J. M. Dimeglio and D. Quere, *Comptes Rendus de l'Academie des Sciences, Serie II*, 1990, **311**, 1473–1478.
- 25 F. Brochard, *Journal of Chemical Physics*, 1986, **84**, 4664–4672.
- 26 D. Quere, J. M. Dimeglio and F. Brochard-wyart, *Revue de Physique Appliquee*, 1988, **23**, 1023–1030.
- 27 D. Quere, J. M. Dimeglio and F. Brochard-wyart, *Science*, 1990, **249**, 1256–1260.
- 28 D. Quere and A. Deryck, *Recherche*, 1994, **25**, 1306–1307.
- 29 L. Rayleigh, *Proc. London Math. Soc.*, 1879, **10**, 4–13.
- 30 S. Middleman, *Modeling Axisymmetric Flows: Dynamics of Films, Jets and Drops*, Academic Press, San Diego, 1995, pp. 241–255.
- 31 L. D. Landau and B. Levich, *Acta Physicochimica USSR*, 1942, **17**, 42–54.
- 32 B. V. Derjaguin, *Acta Physicochimica USSR*, 1943, **20**, 349–352.
- 33 A. D. Rey, *Molecular Crystals and Liquid Crystals*, 1999, **333**, 15–23.
- 34 L. Wang and A. D. Rey, *Liquid Crystals*, 1997, **23**, 93–111.
- 35 Merck, *Technical data sheet for E7 from Merck KGaA*, Darmstadt, Germany.
- 36 L. Bedjaoui, N. Gogibus, B. Ewen, T. Pakula, X. Coqueret, M. Benmouna and U. Maschke, *Polymer*, 2004, **45**, 6555–6560.
- 37 F. M. Leslie, *Quarterly Journal of Mechanics and Applied Mathematics*, 1966, **19**, 357–370.
- 38 J. L. Ericksen, *Physics of Fluids*, 1966, **9**, 1205–1207.
- 39 J. L. Ericksen, *Archive for Rational Mechanics and Analysis*, 1960, **4**, 231–237.
- 40 R. G. Larson, *The Structure and Rheology of Complex Fluids*, Oxford University Press, New York, 1999.
- 41 D. A. Dunmur, in *Physical properties of liquid crystals: Nematics*, ed. D. A. Dunmur, A. Fukuda and G. R. Luckhurst, INSPEC Publications, Herts, UK, 2000, pp. 216–229.
- 42 T. F. Coleman and Y. Y. Li, *Mathematical Programming*, 1992, **56**, 189–222.
- 43 P. G. de Gennes, *The Physics of Liquid Crystals*, Clarendon Press, London, 1974, ch. 5.